ACS NANO

www.acsnano.org

ARTICLE

Zebra-Patterned Stretchable Helical Yarn for Triboelectric Self-Powered Multifunctional Sensing

Yuan Gao,[○] Hu Li,*[,○] Shengyu Chao, Yaqiong Wang, Lanlan Hou, Tonghua Bai, Jie Bai, Xingkun Man, Zhimin Cui, Nü Wang,* Zhou Li,* and Yong Zhao*

Cite This: https://doi.org/10.1021/acsnano.4c03115

ABSTRACT: Smart textiles capable of both energy harvesting and multifunctional sensing are highly desirable for next-generation portable electronics. However, there are still challenges that need to be conquered, such as the innovation of an energy-harvesting model and the optimization of interface bonding between fibers and active materials. Herein, inspired by the spiral structure of natural vines, a highly stretchable triboelectric helical yarn (TEHY) was manufactured by twisting the carbon nanotube/polyurethane nanofiber (CNT/PU NF) Janus membrane. The TEHY had a zebra-stripe-like design that was composed of black interval conductive CNTs and white insulative PU NFs. Due to the different electron affinity, the zebra-patterned TEHY realized a self-frictional triboelectric effect because the numerous microscopic CNT/PU triboelectric interfaces generated an alternating current in the external conductive circuit without extra external friction layers. The helical geometry combined with the elastic PU matrix endowed TEHY with superelastic stretchability and outstanding output stability after 1000 cycles of the stretch−release test. By virtue of the robust mechanical and electrical stability, the TEHY can not only be used as a high-entropy mechanical energy harvester but also serve as a self-powered sensor to monitor the stretching or deforming stimuli and human physiological activities in real time. These merits manifested the versatile applications of TEHY in smart fabrics, wearable power supplies, and human−machine interactions.

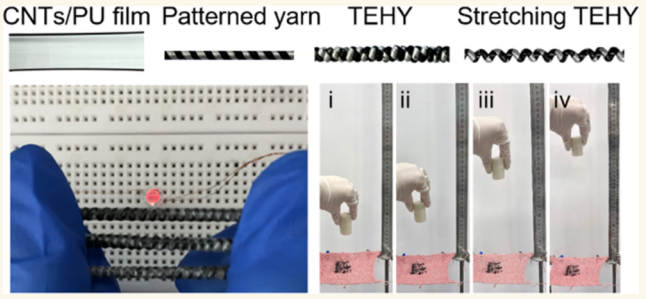

KEYWORDS: *bioinspired, self-friction, self-powered, stretchable helical yarn, multifunctional sensing*

INTRODUCTION

Wearable electronics with high flexibility and stretchability have exerted a considerable impact on human life, ranging from healthcare monitoring and consumer electronics to artificial intelligence and human−machine interactions.[1−6] They exhibited an increasing tendency to become smaller, lightweight, and highly integrated.[7−10] Traditionally, potable electronics use rigid batteries or supercapacitors as energy sources. Such stiff power sources suffered from the drawbacks of bulky volume, heavy weight, limited lifetime, repeated wired charging, and even explosive dangers at moving parts. These limitations seriously hamper their applications in flexible and wearable scenarios. As an emerging energy-harvesting technology, triboelectric nanogenerator (TENG) can continuously convert ambient high-entropy mechanical action into electrical energy.[11−13] Owing to the material availability and environmental friendliness, TENG has shown great application potential for self-powered wearable devices.[14−17]

Currently, most of the TENGs are assembled by metal or polymer films as positive and negative friction layers.[18,19] Although such film devices can be flexible or bendable, they usually have poor stretchability, low damage tolerance, poor air permeability, and low integrated capability with fabrics. These defects impede their wide application in wearable textile electronics. As the most basic building block in clothes, fibers can be easily woven into textiles, which makes it a preferred candidate for constructing stretchable and wearable electronic devices.[20−25] Recently, helical fibers with high stretchability that can alleviate the local maximum strain through the nonplanar

Received: March 6, 2024
Revised: May 26, 2024
Accepted: June 10, 2024

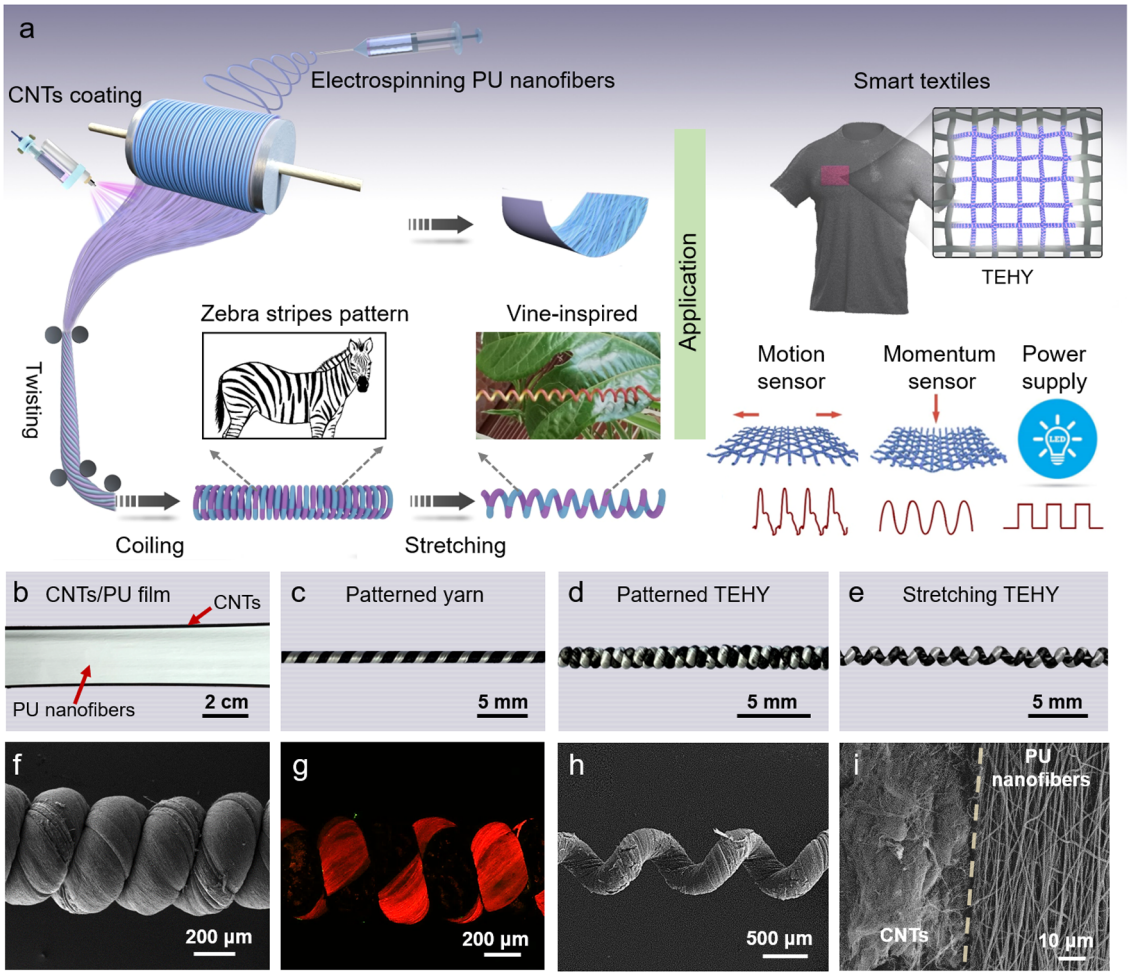

Figure 1. Vine-inspired structure design and manufacture process of the zebra-patterned TEHY. (a) Preparation scheme of TEHY. Inspired by vines, the TEHY with a multiscale helical structure was fabricated by successive electrospinning, CNT coating, and twisting process. The photograph of (b) PU strip coated with CNTs on the one side, (c) twisted CNT/PU yarn with interval black−white zebra pattern, (d) overtwisted helical TEHY yarn, and (e) yarn structure under stretch state. (f) Confocal and (g) SEM images of the zebra-patterned helical yarn. The pattern can be clearly observed with regular alternation structures. (h) TEHY structure under the stretch state. (i) High-magnification of the junction between CNTs and PU NFs.

motion of the coils have been developed. This feature endows helical yarn with higher durability and stretchability.[26−32] Some researchers prepared helical triboelectric yarn via encapsulating conductive metal wires (such as copper, steel, silver, etc.) by elastic polymer shells.[33−35] However, intrinsic rigid metals limited their integration with traditional textiles. Additionally, the interface binding force between elastic matrix and rigid conductive metals is often mismatched, which results in the peeling off of active materials during deformation and finally affects the device stability.[36,37] Therefore, on the premise of ensuring the flexibility and stretchability of the helical yarn, how to optimize the interface bonding force between the substrate and the electroactive material to improve the stability is the key to realizing the functional application of triboelectric fibers.[38]

Furthermore, optimizing the friction mode of triboelectric layers also plays an important role in promoting the performance of fiber-based TENG. The working mechanism of fiber TENG is based on the coupling of triboelectrification and electrostatic induction. Triboelectricity generated at the friction interface when two independent objects repeatedly contacted and separated from each other.[39−41] If the friction process can accomplish the contact−separation motion by itself and generate triboelectricity on an all-in-one device, it will bring a power supply strategy for smart wearable devices.

Herein, we developed a spiral vine-inspired superelastic triboelectric helical yarn (TEHY), which was fabricated by overtwisting the carbon nanotube (CNT) and polyurethane nanofiber (PU NF) Janus membrane. The interval black conductive CNTs and white insulative PU NFs formed a zebra strip pattern that generated an electric potential difference between CNTs and PU NFs during the stretching process. Owing to its fast response time and high stretchability, the zebra-patterned TEHY can monitor human motions as strain sensors. Furthermore, after the TEHY is woven into textiles, the TEHY cloth can act as a mechanical sensor to pinpoint the impact or measure the momentum of the object. The zebra-patterned TEHY brought a self-frictional strategy to realize power generation and conversion, indicating versatile application prospects in wearable electronics and related fields.

RESULTS AND DISCUSSION

Bioinspired Designing of the Superstretchable TEHY with Mechanical−Electrical Stability. In nature, spiral plant vines can effectively alleviate the external stretch force and

https://doi.org/10.1021/acsnano.4c03115
ACS Nano XXXX, XXX, XXX−XXX

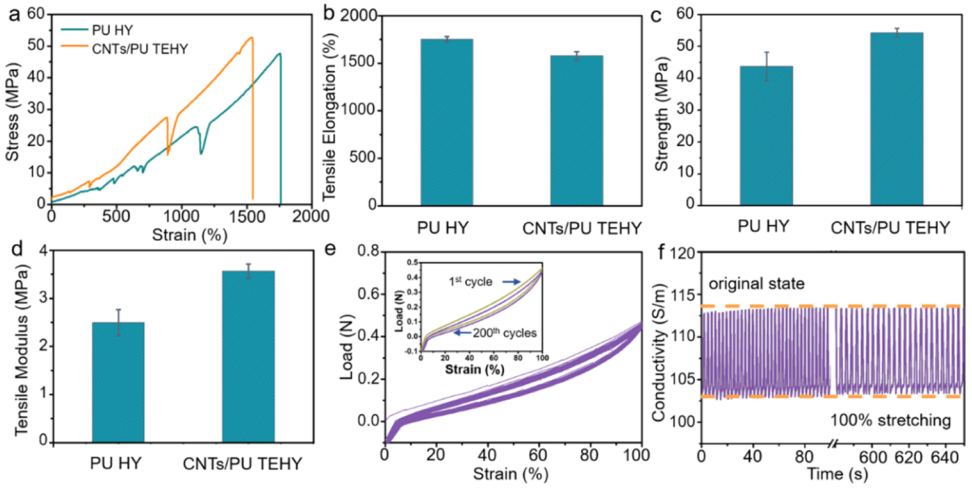

Figure 2. Mechanical properties of the PU helical yarn (HY) and TEHY. (a) Stress curve, (b) breaking strength, (c) elongation, and (d) tensile modulus of the pure PU helical yarn and TEHY. The TEHY exhibited excellent stretchability and elasticity. (e) Loading−unloading curves under 100% tensile strain for 200 cycles and (f) conductivity variation curves. The curves can preferably recover during the deformation process showing good reproducibility and stability.

provide shock absorption to maintain structural stability. Inspired by the spiral vine, we designed a zebra-patterned TEHY by overtwisting the CNTs and electrospun PU NFs Janus film. Figure 1a schematically displayed a three-step fabrication process of the superstretchable TEHY. First, the PU NFs substrate film was prepared by electrospinning. To endow the conductivity and stability, a black CNT suspension was sprayed on one side of the white PU NF film to form a CNT/PU NF Janus membrane (Figure 1b). Then, the CNT/PU NF Janus film was twisted into a straight yarn with an alternating black−white zebra strip pattern (Figures 1c and S1). Finally, the straight yarn was further overtwisted into a spring-like TEHY, which had neat loops with a tight arrangement (Figure 1d,e). The zebra strip pattern of the TEHY was clearly revealed by the confocal microscopy. The red strip was PU NFs dyed by Dil, and the dark strip was CNTs without dyeing (Figure 1f,g). The related microscopic morphology of the TEHY was illustrated by scanning electron microscopy (SEM; Figure 1h,i). TEHY exhibited a uniform wavy structure under 100% tensile strain. The CNTs clung to the PU NF surface, which was like vines on a tree trunk. With the sandwich structure (PU-CNTs-PU), the winding CNTs can be locked in PU layers (Figure S2). It can be seen that the CNTs were tightly combined with the PU NF substrate, which improved the mechanical stability of the zebra-patterned TEHY.

Owing to the pristine elastic PU polymer and the multiscale helical structures, the CNT/PU TEHY exhibited high mechanical properties with ultrahigh stretchability. It is seen that the tensile elongation, strength, and Young's modulus of the CNT/PU TEHY are 1580%, 54.3, and 3.6 MPa, respectively, while the control group of PU helical yarn (HY) displays 1750%, 43.8, and 2.5 MPa, respectively (Figure 2a−d). Compared to PU HY, the elongation of TEHY decreased slightly (Figure S3), while the strength and Young's modulus improved due to the composite of the high-strength CNTs. During the elongation of the spiral structure, the nonplanar motion of the coils can effectively inhibit the stress concentration of the rigid conductive CNT layer to uniform the local maximum strain, which endows the TEHY with high stretchability and tensile strength.[42,43] From the overlapped variations of the loading−unloading curves under 100% tension, the TEHY maintained 96.4% strain after 200 cycles of the stretch−release test, further manifesting good mechanical and structural stability (Figure 2e). To confirm the synergy between mechanical and electrical properties, the electromechanical properties of TEHY were characterized under the dynamic tensile strain. With the tensile strain stepwise increasing by 100%, the TEHY resistance gradually increased from 66.8 to 78.2 Ω (Figure S4). Both resistance and structure can complete recovery during the stretch−release cycles (Figure S5). It proved that the resilience of TEHY was derived from the flexible PU substrate and hierarchical spiral structure. In addition, the relationship between elongation and conductivity was an important indicator to evaluate the yarn performance. Because the spiral structure can disperse the stress distribution, the conductivity variation of the TEHY was comparatively small from 118 to 93.3 S/m in the first 400% stretching (Figure S6). Actually, in practical applications, the 100% tensile strain can basically satisfy the deformation scenes of wearable electronics. The mechanical−electrical synergy of the TEHY was also optimal under this tensile state. Hence, the electrical conductivity of TEHY was tested under 100% stretching with 200 cycles. As displayed in Figure 2f, the TEHY exhibited good electrical recovery because the CNTs possessed a continuous conductive path inside the helical yarn. The hierarchical structure with a winding-locked conductive layer not only ensured the integrity of the conductive pathway under deformation but also enhanced the conductive and mechanical reliability. Therefore, TEHY could be used as an ideal candidate for stretchable sensors. Furthermore, this strategy endowed the yarn with excellent mechanical and electrical properties just by incorporating a small amount of CNTs (6.15 wt %) (Figure S7), which provided an efficient and low-cost direction for the preparation of self-powered wearable devices.

Output Performance and Working Principle of TEHY. In addition to the excellent mechanical properties, the zebra-patterned TEHY exhibited a self-frication triboelectric power generation function. Due to the different electron affinity between CNTs and PU, TEHY generated electric potential via the self-friction of numerous microscopic CNT/PU interfaces during the stretch−release process. To further improve the electromechanical stability of TEHY, the yarn was encapsulated

https://doi.org/10.1021/acsnano.4c03115
ACS Nano XXXX, XXX, XXX−XXX

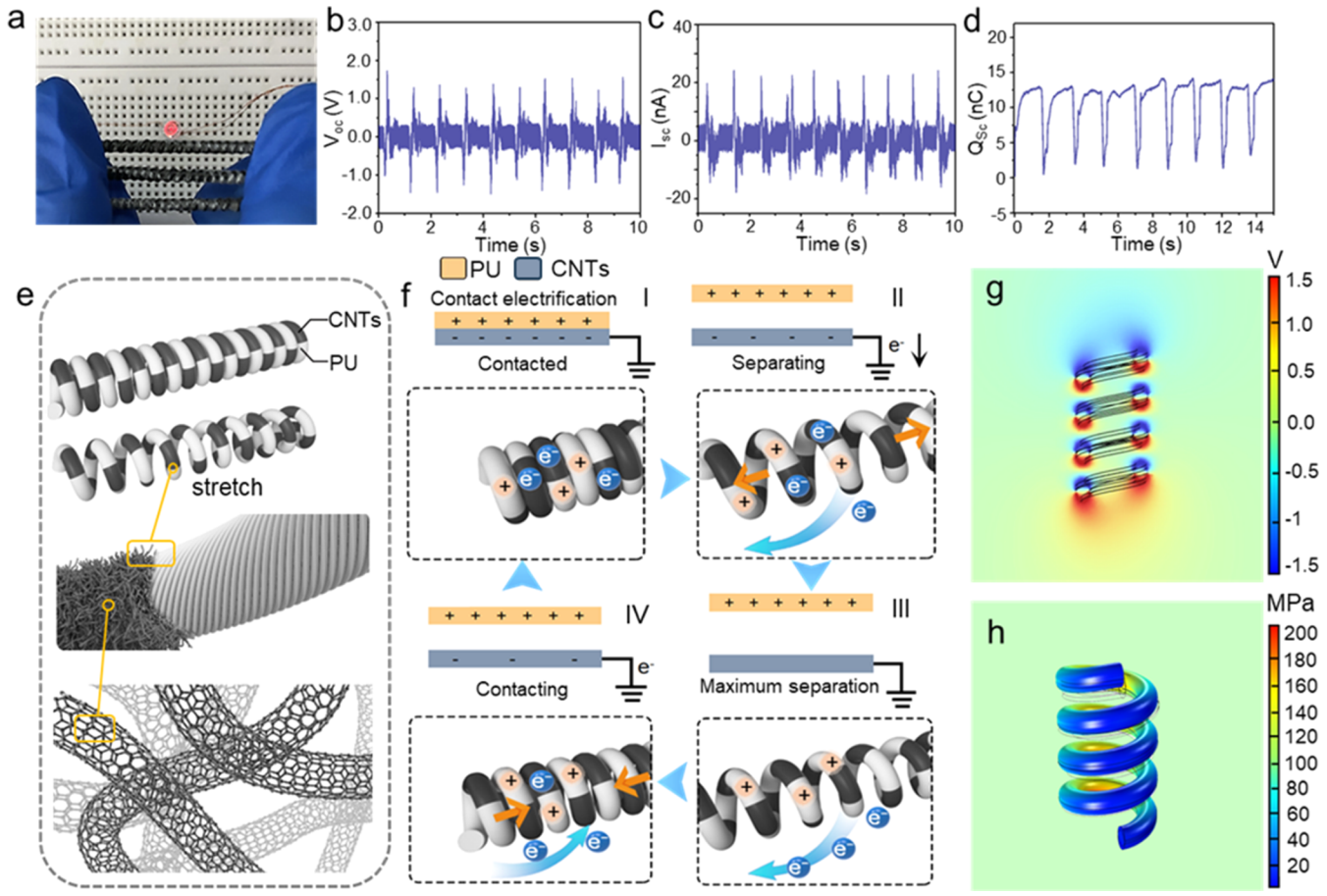

Figure 3. Triboelectric output performance and working principle of the zebra-patterned TEHY. (a) Light up the LED by stretching the TEHY device. (b) Open-circuit voltage, (c) short-circuit current, and (d) short-circuit charge signals of the TEHY. (e) Macroscopic and microscopic structure diagram of TEHY. (f) Working mechanism of the single-electrode TEHY. (g) COMSOL simulation of the electric potential distribution and (h) stress distribution during the stretch process. The stress distribution of the helical structure is uniform, which enhances the mechanical durability of the TEHY.

with silicone rubber (Ecoflex). The TEHY enabled to light the light-emitting diode (LED) during the stretch−recover process (Figure 3a). We fixed one side of the yarn to the probe of the oscilloscope. The other side was fixed on a linear motor. With the motor moving, the helical coils of TEHY were periodically contacted and separated. The output performance of the TEHY (2.5 cm in length and 1.2 mm in diameter) is quantitatively evaluated in Figure 3b−d. The open-circuit voltage (V_{OC}), short-circuit current (I_{SC}), and short-circuit charge transfer (Q_{SC}) are about 1.5 V, 20 nA, and 13 nC, respectively. Encapsulated with other elastic outer layers such as a very high bond (VHB) tape, TEHY still exhibited excellent mechanical−electrical integration (Figures S8 and S9). Due to the protection of the encapsulation layer, TEHY showed washability and stable electric output after water immersion (Figure S10).

The self-frictional triboelectric working principle of the zebra-patterned TEHY is based on the coupling of contact electrification and electrostatic induction, which is manifested in Figure 3e,f. Originally, the full contact between PU and CNTs generates surface charges at their interface due to contact electrification (Figure 3f-I). Electrons are injected from PU to the CNT surface because PU is more triboelectrically positive than CNTs, according to the tested triboelectric series. At this moment, the opposite equivalent charges are fully balanced and no electrons flow in the external circuit. Because PU is an insulating material enabling the generated positive charges to be preserved on its surface for a long time. When PU begins to separate from CNTs, it results in the decrease of the induced negative charges on CNTs, and the potential difference between CNTs and ground drives the electrons to flow from CNTs to the ground through the external circuit (Figure 3f-II). When PU fully separates from CNTs with maximum separation, the induced negative charges on CNTs are fully screened with no electric output in the external circuit (Figure 3f-III). When PU moves back to the CNT surface, the induced negative charges on CNTs increase, driving the electrons to flow from the ground to CNTs again through the external circuit. When PU recovers full contact with CNTs, the TEHY returns to its original state (Figure 3f-IV). The periodic contact and separation between PU and CNTs generate the periodic alternating current and realize the energy conversion between mechanical energy and electricity. A full cycle of the electricity generation process for TEHY is completed. To further describe the mechanism of energy conversion, the electric potential distribution between PU NFs and CNTs is simulated by COMSOL software (Figure 3g). In order to simplify the calculation, the device is divided into three polarization parts, and a static capacitance model is used in the electrical simulation. To complete the finite element analysis, the polarization potential of 1.5 V, a relative dielectric constant of 4, a style modulus of 3.5 MPa, a Poisson ratio of 0.4, and a density of 1.7 kg/m^3 are added to the TEHY. It is worth mentioning that the simulation uses static electrical and

https://doi.org/10.1021/acsnano.4c03115
ACS Nano XXXX, XXX, XXX−XXX

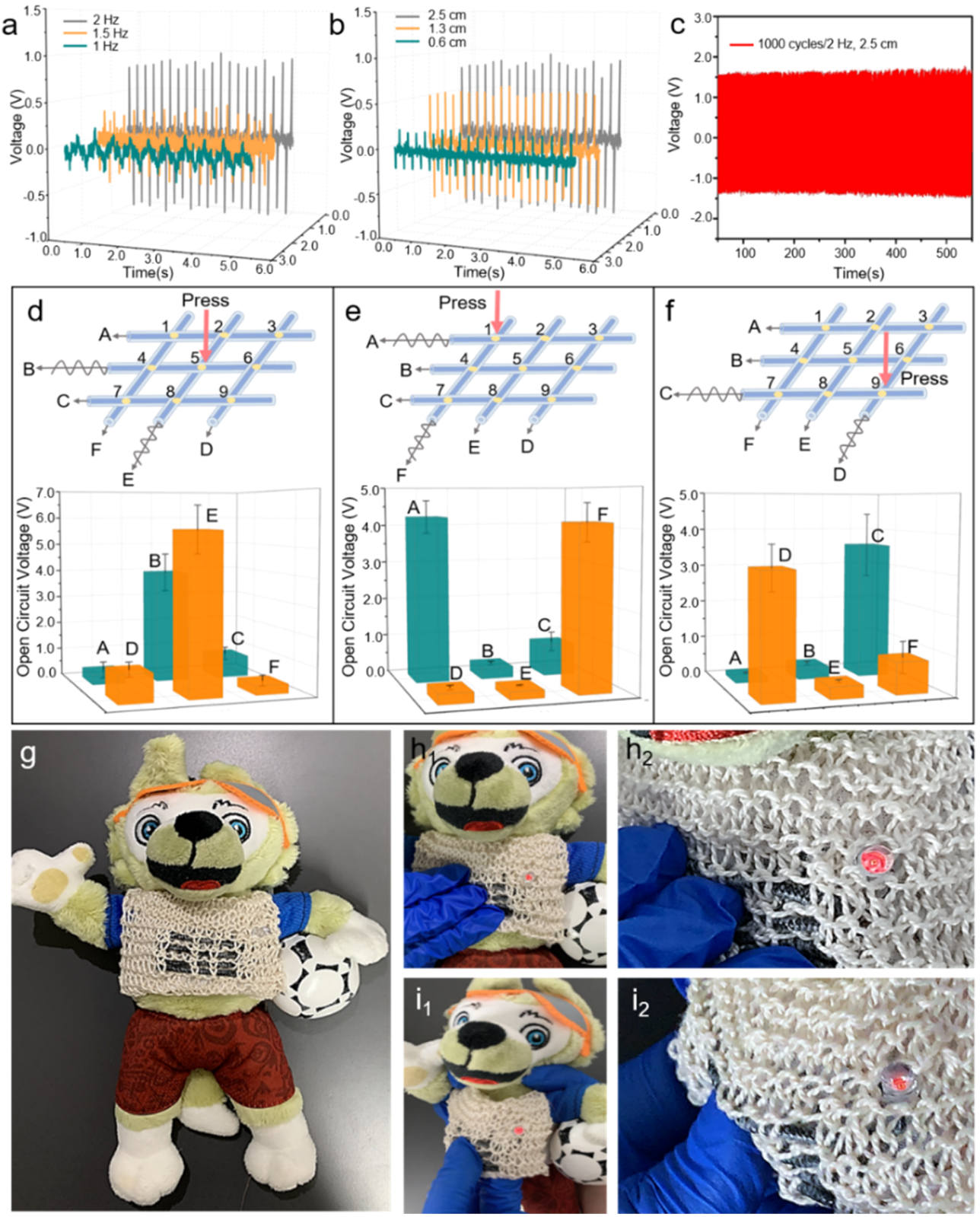

Figure 4. Triboelectric output performance and applications of the knitted TEHYs textile. The output voltage increased with (a) the stretching frequency and (b) the yarn length. (c) Highly stable output voltage during the periodical stretch−recover process. (d−f) A 3 × 3 TEHY textile (cross section numbered from 1 to 9) was used as the pressure sensor to identify the press positions. The corresponding triboelectric signals with pressing positions of (d) 5, (e) 1, and (f) 9. Press position can be accurately identified by monitoring the triboelectric signal strength. (g) TEHYs were woven into the athletes' clothes. The self-powered TEHYs can light up the LED with (h) hitting or pushing and (i) pulling the player's clothes. In the sports competition, the violation operation of athletes can be monitored in a visual mode.

https://doi.org/10.1021/acsnano.4c03115
ACS Nano XXXX, XXX, XXX−XXX

mechanical models, which can be considered consistent with real conditions at static and low speeds and without external interference. The contour clearly showed that a potential difference existed between PU NFs and CNTs when they contacted with each other. The potential difference drives free electrons to flow in the external circuit. At the same time, mechanics simulation was also performed to show the stress distribution along the TEHY during the stretch−release process (Figure 3h). It showed that the helical structure can effectively reduce the slip and deformation of a single fiber, disperse stress, and enhance its mechanical durability during repetitive stretch and release. In the TEHY, the elastic PU NF substrate played a fundamental role in maintaining excellent tensile recovery performance, while the CNTs were firmly winding-locked into the twisted yarn, which avoided CNTs peeling off from the yarn matrix during the deformation process and ensured the electrical stability of the material. The multiscale synergistic effect endowed the TEHY with excellent mechanical and electrical properties.

Triboelectric Performance of TEHY. The above results have demonstrated that zebra-patterned TEHY was able to generate an alternating electric current based on the self-frictional triboelectric mechanism. The electrical properties of TEHY can be influenced by the yarn length and the stretching frequency. The impact of related parameters on the output performance is shown in Figure 4a,b. During the stretch−recovery process on a 2.5 cm long TEHY, the output voltage displayed an obvious increase with the frequency increasing from 1 Hz, 1.5 to 2 Hz. The corresponding peak voltages were 0.20, 0.42, and 0.89 V, respectively. Then, we further investigated the influence of the TEHY length on the power generation performance at a stretching frequency of 2 Hz. The open-circuit voltage raised from 0.3 to 0.63 V and then to 0.97 V when the yarn length increased from 0.6 to 1.3 and to 2.5 cm, respectively. A longer yarn length meant a larger effective contact−separation area of CNTs and PU NFs, which, in turn, increased the output voltage. Additionally, the TEHY diameters can also influence the output performance. The effective contact−separation area between PU nanofibers and CNTs increased with the TEHY diameters, which in turn increased the V_{oc} (Figure S11). Notably, the output voltage was almost unchanged with the change in mass ratio of CNTs (Figure S12). It was because the existing CNTs already formed an intact conductive network layer. The addition of more CNTs has a negligible impact on the conductivity. TEHY also has an outstanding stable output during 1000 cycles of stretch−release test at 2 Hz and 100% stretching quantity (Figure 4c). The real-time curve had the same variation trend and showed excellent repeatability of resistances and a low degree of hysteresis (Figure S13). The almost unchanged output voltage curves proved the stability of the TEHY. With the increment of tensile strains from 100 to 400%, TEHY can still maintain an effective electrical output, which slightly decreased from 1.58 to 1.12 V (Figure S14). Although the TEHY resistance increased and the stretching frequency decreased with elongation, the PU and CNTs can still achieve the contact−separation process with the uncoiling−coiling of the helical structure, which ensures triboelectric generation. Further increasing the tensile strain, TEHY would be completely straightened (Figure S15). Obviously, PU and CNTs alternately appeared on the straight yarn, which cannot realize the contact−separation process to generate self-friction output.

Applications of TEHY Textiles. Considering the portability, miniaturization, stretchability, and triboelectric ability, TEHY is capable of serving as self-powered active sensors to monitor human motions and interact with body language information translation. Herein, TEHY was first used to identify the gesture. Different gestures can generate characteristic triboelectric signals and represent the corresponding warning information. Five TEHYs (2 cm in length) were stuck on knuckles and connected to five channels of an oscilloscope. The triboelectric signal combinations were realized by adjusting the finger motion combinations. For example, in the swimming scene, keeping five fingers still means the signal "paused"; simultaneously bending the thumb and forefinger expresses the signal "OK"; simultaneously bending five fingers indicates the alarm "danger" (see Figure S16). This interactive information and translation proved the successful demonstration in swimming teaching or other scenes for students unable to speak. It also can find values for sign language or remote operation, providing real-time alerts and health monitoring for workers.

In addition to monitoring the finger motion, the TEHY can be further knitted into textiles to detect the pressure and pinpoint the position. Six TEHYs were knitted into an intersected array (3 × 3) with nine triboelectric intersections, which can serve as nine independent pressure sensing units in a plane (Figure 4d−f). When applying pressure on an intersection position, the two intersected TEHYs will generate two triboelectric signals, respectively, which are much stronger than other crosstalk signals without press force. By identifying these two stronger triboelectric signals, we can accurately locate the pressure positions. As shown in Figure 4d, when pressed on the intersection position 5, yarn B interacted with yarn E. Then, two triboelectric voltage signals were generated in real time from *B* (3.9 V) and *E* (5.6 V). This function can be further confirmed by pressing the other optional intersection positions, for example, positions 1 (Figure 4e) and 9 (Figure 4f). By analyzing the output voltage signals, we can accurately decode the pressure positions. With this function, the knitted TEHY can be used as a touch positioning sensor textile.

In sports games, referees need to follow the high-speed moving athletes all of the time to supervise their violations. Referees tend to overlook some inconspicuous fouls under high physical exertion. If the crude behavior can be highlighted, it will provide great convenience for referees. Herein, we demonstrated the feasibility of using TEHY textiles to convert physical contact into visual light signals. Four TEHYs (4 cm in length) were knitted in the shirt of a football player doll (Figure 4g). A light-emitting diode (LED) was connected to the TEHYs. When an athlete was hit, pushed, or pulled by others, the instantaneous mechanical energy was converted into electrical energy to immediately light up the warning LED on athletes' clothes, which make it easier for referees to judge the violations (Figure 4h,i and Movie S1).

In addition to motion judgment functions, the TEHYs can be also knitted into fabrics to qualitatively evaluate the weight or height of falling objects. When an object freely falls to the TEHYs' fabric (9 cm^2 square), the knitted TEHYs net would be stretched and converted into characteristic triboelectric signals related to the weight and height, i.e., the kinetic energy of the object. With the object shape fixed, the weight or height can be accurately qualitatively identified relied on the strength of triboelectric signals by controlling a single variable. As shown in Figure 5a, a plastic block (5 g) fell above the TEHY textile at

https://doi.org/10.1021/acsnano.4c03115
ACS Nano XXXX, XXX, XXX−XXX

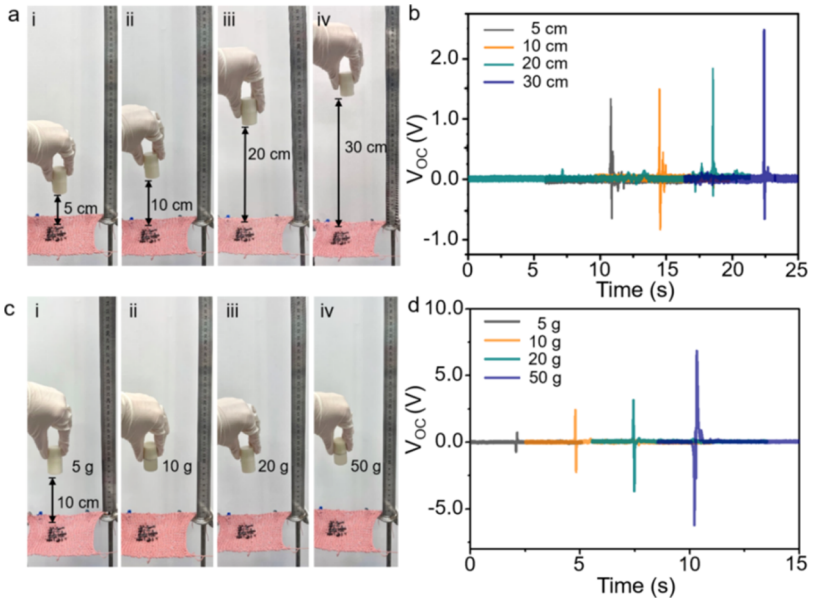

Figure 5. Knitted TEHY smart textile is used to qualitatively recognize the height and weight of an object. (a) Plastic block (5 g) falls from the height of 5, 10, 20, and 30 cm, respectively. (b) Output voltage curves at different falling heights. (c) Plastic blocks with different weights (5, 10, 20, and 50 g) fall at the same height (10 cm). (d) Output voltage curves of different object weights.

different heights: 5 cm (i), 10 cm (ii), 20 cm (iii), and 30 cm (iv). Results indicated that the output voltages of the fabric showed a positive correlation with the falling heights (Figure 5b). Subsequently, the blocks with different weights (5, 10, 20, and 50 g) were fixed above the fabric at the same height (10 cm) and dropped onto the TEHY textile by free fall. The electric output also showed a positive correlation with the object weights (Figure 5c,d). These demonstrations proved the feasibility of TEHYs as the momentum recognition device.

CONCLUSIONS

In summary, a vine-inspired spiral superstretchable self-frictional triboelectric helical yarn was designed by overtwisting the CNT and PU NF Janus composite films. The twisted yarn possessed an interesting zebra strip pattern consisting of alternating black conductive CNTs and white insulative PU NFs. The electron affinity difference between CNTs and PU NFs produced an electric potential difference on the CNT/PU contact interfaces that could effectively convert mechanical energy into electricity under the combined action of numerous CNT/PU contact interfaces within the yarn structure. The zebra-patterned triboelectric helical yarn showed multifunctional self-powered sensing applications, such as interactive gesture identification, precise localization, qualitative identification, and visual judgment of sports violations. It is predictable that the triboelectric helical yarn will find broader applications in smart fabrics, wearable power supplies, and human−machine interaction.

MATERIALS AND METHODS

Materials. Polyester polyurethane (PU, CAS number: 68084-39-9; Sigma-Aldrich), *N*,*N*-dimethylformamide (DMF, AR, Beijing Fine Chemical Co., Ltd.), tetrahydrofuran (THF, AR, Beijing Fine Chemical Co., Ltd.), ethanol (AR, Beijing Fine Chemical Co., Ltd.), single-walled carbon nanotubes, the average diameter is 1−2 nm (CNTs, XFNANO, Inc. XFS22), and silicone rubber (Ecoflex Supersoft 00−30, Smooth-On, Inc.) were used without further treatment.

Preparation of PU Nanofiber (PU NF) Membrane by Electrospinning. The PU pellets were dissolved in a mixture solution of DMF and THF (1:1, mass ratio) at room temperature to prepare the 7 wt % PU electrospinning solution (Figure S17). The PU solution was subsequently electrospun at 17 kV, 20 cm tip-to-collector distance, 25 °C, and 35% RH on a Nafiber SR-100 electrospinning instrument. The electrospun PU NF membrane was collected by a drum collector at 1200 rpm.

Fabrication of the Superelastic, Conductive, and Zebra-Patterned Helical Yarn. CNTs were dispersed in ethanol under stirring for 2 h and ultrasonic treatment for 2 h to prepare the CNT dispersion liquid. Then, the CNT suspension was sprayed onto one side of the PU nanofiber membrane and formed a Janus CNT/PU film. The CNT/PU film was cut into ribbons with a width of 2 cm. Then, the ribbons were twisted into a straight yarn driven by a motor. Due to the involution structure of the Janus membrane, it exhibited a black−white (CNT/PU) zebra strip pattern. With a further overtwisting process, the straight yarn was transformed into the coiled helical yarn. Afterward, the yarn was soaked in liquid silicone rubber and dried at room temperature to coat an elastomeric protective layer.

Characterization and Measurement. Field-emission scanning electron microscopy (SEM, Quanta 250 FEG) and confocal laser scanning microscopy (Olympus, FV1000) were used to characterize the yarn structures. The CNT contents in CNT/PU helical yarn were investigated by a thermogravimetric analysis (TGA) analyzer with a heating rate of 10 °C/min in an N_2 atmosphere. The mechanical properties were determined by a universal mechanical testing machine (SHIMADZU, AGS-X 1 KN) at a strain rate of 10 mm/s. The electrical output of the yarn (V_{OC}, I_{SC}, and Q_{SC}) was measured by a Keithley 6517 electrometer and oscilloscope (LeCroy HDO6104). The TEHY was connected to an oscilloscope. A wire from the continuous CNT layer was connected to the positive electrode of the oscilloscope. The negative electrode of the oscilloscope was grounded.

Measurement of Strain Sensors. The helical yarn-based pressure sensing array was fabricated by 3 × 3 sensing units. Subsequently, each sensing unit was connected to an oscilloscope. The sensing array generated nine pressure detection points based on the cross points of two overlapping yarns. The V_{OC} of six channels was synchronously measured by the electrometer. Based on the same principle, we wove the helical yarns into the fabric sensors and recorded the corresponding V_{OC} signals.

https://doi.org/10.1021/acsnano.4c03115
ACS Nano XXXX, XXX, XXX−XXX

ASSOCIATED CONTENT

Supporting Information

The Supporting Information is available free of charge at https://pubs.acs.org/doi/10.1021/acsnano.4c03115.

Instantaneous mechanical energy was converted into electrical energy to immediately light up the warning LED on athletes' clothes, which makes it easier for referees to judge the violations (MP4)

SEM of the patterned TEHY, the coated CNTs on the PU substrate, and the three oriented PU NFs; the micromorphology of the interface between elastic PU NFs and CNTs; the morphology and diameter distribution of different mass fractions of polyurethane 3 solutions after electrospinning (PDF)

AUTHOR INFORMATION

Corresponding Authors

Hu Li − *Beijing Key Laboratory of Micro-nano Energy and Sensor, Beijing Institute of Nanoenergy and Nanosystems, Chinese Academy of Sciences, Beijing 101400, P. R. China; Department of Biomedical Engineering, City University of Hong Kong, Hong Kong 999077, P. R. China;* Email: huli23@cityu.edu.hk

Nü Wang − *Key Laboratory of Bioinspired Smart Interfacial Science and Technology of Ministry of Education School of Chemistry, Beihang University, Beijing 100191, P. R. China;* orcid.org/0000-0002-8722-0596; Email: wangn@buaa.edu.cn

Zhou Li − *Beijing Key Laboratory of Micro-nano Energy and Sensor, Beijing Institute of Nanoenergy and Nanosystems, Chinese Academy of Sciences, Beijing 101400, P. R. China; School of Nanoscience and Technology, University of Chinese Academy of Sciences, Beijing 100049, P. R. China;* orcid.org/0000-0002-9952-7296; Email: zli@binn.cas.cn

Yong Zhao − *Key Laboratory of Bioinspired Smart Interfacial Science and Technology of Ministry of Education School of Chemistry, Beihang University, Beijing 100191, P. R. China; Chemical Engineering College, Inner Mongolia University of Technology, Hohhot 010051, P. R. China;* orcid.org/0000-0002-2545-1620; Email: zhaoyong@buaa.edu.cn

Authors

Yuan Gao − *School of Machinery and Automation, Weifang University, Weifang 261061, P. R. China; Key Laboratory of Bioinspired Smart Interfacial Science and Technology of Ministry of Education School of Chemistry, Beihang University, Beijing 100191, P. R. China*

Shengyu Chao − *School of Nanoscience and Technology, University of Chinese Academy of Sciences, Beijing 100049, P. R. China*

Yaqiong Wang − *Key Laboratory of Bioinspired Smart Interfacial Science and Technology of Ministry of Education School of Chemistry, Beihang University, Beijing 100191, P. R. China*

Lanlan Hou − *Key Laboratory of Bioinspired Smart Interfacial Science and Technology of Ministry of Education School of Chemistry, Beihang University, Beijing 100191, P. R. China*

Tonghua Bai − *Key Laboratory of Bioinspired Smart Interfacial Science and Technology of Ministry of Education School of Chemistry, Beihang University, Beijing 100191, P. R. China*

Jie Bai − *Chemical Engineering College, Inner Mongolia University of Technology, Hohhot 010051, P. R. China;* orcid.org/0000-0002-7662-8238

Xingkun Man − *Center of Soft Matter Physics and Its Applications, School of Physics and Nuclear Energy Engineering, Beihang University, Beijing 100191, P. R. China;* orcid.org/0000-0003-4266-1539

Zhimin Cui − *Key Laboratory of Bioinspired Smart Interfacial Science and Technology of Ministry of Education School of Chemistry, Beihang University, Beijing 100191, P. R. China*

Complete contact information is available at: https://pubs.acs.org/10.1021/acsnano.4c03115

Author Contributions

○Y.G. and H.L. contributed equally to this work. Y.G., H.L., N.W., Z.L., and Y.Z. conceived the idea and contributed to the design of experiments. Y.G. fabricated the TEHY and wrote the manuscript. Y.G. and H. L. performed the mechanical and electrical experiments. S.C. realized the simulation. Y.G., L.H., and Y.W. processed data. J.B., X.M., Z.C., N.W., Z.L., and Y.Z. guided reader design and troubleshooting. N.W., Z. L., and Y.Z. supervised the project. The manuscript was written through contributions of all authors. All authors have given approval to the final version of the manuscript.

Notes

The authors declare no competing financial interest.

ACKNOWLEDGMENTS

The authors gratefully acknowledge the financial support by the National Natural Science Foundation of China (21975007 and T2125003), the Shandong Provincial Natural Science Foundation of China (ZR2021QB210), the Beijing Natural Science Foundation (2232054, JQ20038, and L212010), and the Fundamental Research Funds for the Central Universities (YWF-22-K-101, E0EG6802X2).

REFERENCES

(1) Lipomi, D. J.; Vosgueritchian, M.; Tee, B. C.; Hellstrom, S. L.; Lee, J. A.; Fox, C. H.; Bao, Z. Skin-like pressure and strain sensors based on transparent elastic films of carbon nanotubes. *Nat. Nanotechnol.* **2011**, *6*, 788−792.

(2) Qi, D.; Liu, Z.; Liu, Y.; Leow, W. R.; Zhu, B.; Yang, H.; Yu, J.; Wang, W.; Wang, H.; Yin, S.; Chen, X. Suspended wavy graphene microribbons for highly stretchable microsupercapacitors. *Adv. Mater.* **2015**, *27*, 5559−5566.

(3) Zhou, B.; Chen, Y.; Liu, Y.; Xie, R.; Du, Q.; Zhang, T.; Shen, Y.; Zheng, B.; Li, S.; Wu, J.; Zhang, W.; Huang, W.; Huang, X.; Huo, F. Repurposed Leather with Sensing Capabilities for Multifunctional Electronic Skin. *Adv. Sci.* **2019**, *6*, No. 1801283.

(4) Gong, S.; Schwalb, W.; Wang, Y.; Chen, Y.; Tang, Y.; Si, J.; Shirinzadeh, B.; Sheng, W. A wearable and highly sensitive pressure sensor with ultrathin gold nanowires. *Nat. Commun.* **2014**, *5*, No. 3132.

(5) Wei, X.; Li, H.; Yue, W.; Gao, S.; Chen, Z.; Li, Y.; Shen, G. A high-accuracy, real-time, intelligent material perception system with a machine-learning-motivated pressure-sensitive electronic skin. *Matter* **2022**, *5*, 1481−1501.

(6) Kim, D. H.; Bae, J.; Lee, J.; Ahn, J.; Hwang, W. T.; Ko, J.; Kim, D., II. Porous nanofiber membrane: rational platform for highly sensitive thermochromic sensor. *Adv. Funct. Mater.* **2022**, *32*, No. 2200463.

(7) Li, P.; Zhang, Y.; Zheng, Z. Polymer-assisted metal deposition (PAMD) for flexible and wearable electronics: principle, materials, printing, and devices. *Adv. Mater.* **2019**, *31*, No. 1902987.

(8) Yu, X.; Xie, Z.; Yu, Y.; Lee, J.; Vazquez-Guardado, A.; Luan, H.; Ruban, J.; Ning, X.; Akhtar, A.; Li, D.; Ji, B.; Liu, L.; Sun, R.; Cao, J.; Huo, Q.; Zhong, Y.; Lee, C.; Kim, S.; Gutruf, P.; Zhang, C.; Xue, Y.;

Guo, Q.; Chempakasseril, A.; Tian, P.; Lu, W.; Jeong, J.; Yu, Y.; Cornman, J.; Tan, C.; Kim, B.; Lee, K.; Feng, X.; Huang, Y.; Rogers, J. A. Skin-integrated wireless haptic interfaces for virtual and augmented reality. *Nature* **2019**, *575*, 473−479.
(9) Lee, S.; Franklin, S.; Hassani, F. A.; Yokota, T.; Nayeem, M. O. G.; Wang, Y.; Leib, R.; Cheng, G.; Franklin, D. W.; Someya, T. *Science* **2020**, *370*, 966−970.
(10) Cuthbert, T. J.; Hannigan, B. C.; Roberjot, P.; Shokurov, A. V.; Menon, C. HACS: Helical Auxetic Yarn Capacitive Strain Sensors with Sensitivity Beyond the Theoretical Limit. *Adv. Mater.* **2023**, *35*, No. 2209321.
(11) Wang, Z. L. Triboelectric nanogenerators as new energy technology for self-powered systems and as active mechanical and chemical sensors. *ACS Nano* **2013**, *7*, 9533−9557.
(12) Nie, J.; Wang, Z.; Ren, Z.; Li, S.; Chen, X.; Wang, Z. L. Power generation from the interaction of a liquid droplet and a liquid membrane. *Nat. Commun.* **2019**, *10*, No. 2264.
(13) Dong, C.; Leber, A.; Yan, D.; Banerjee, H.; Laperrousaz, S.; Gupta, D. T.; Shadman, S.; Reis, M. P.; Sorin, F. 3D stretchable and self-encapsulated multimaterial triboelectric fibers. *Sci. Adv.* **2022**, *8*, No. eabo0869.
(14) Dong, K.; Wang, Y. C.; Deng, J.; Dai, Y.; Zhang, S. L.; Zou, H.; Gu, B.; Sun, B.; Wang, Z. L. A highly stretchable and washable all-yarn-based self-charging knitting power textile composed of fiber triboelectric nanogenerators and supercapacitors. *ACS Nano* **2017**, *11*, 9490−9499.
(15) Xiong, J.; Cui, P.; Chen, X.; Wang, J.; Parida, K.; Lin, M. F.; Lee, P. S. Skin-touch-actuated textile-based triboelectric nanogenerator with black phosphorus for durable biomechanical energy harvesting. *Nat. Commun.* **2018**, *9*, No. 4280.
(16) Wang, J.; Li, S.; Yi, F.; Zi, Y.; Lin, J.; Wang, X.; Xu, Y.; Wang, Z. L. Sustainably powering wearable electronics solely by biomechanical energy. *Nat. Commun.* **2016**, *7*, No. 12744.
(17) Meng, X.; Cai, C.; Luo, B.; Liu, T.; Shao, Y.; Wang, S.; Nie, S. Rational Design of Cellulosic Triboelectric Materials for Self-Powered Wearable Electronics. *Nano-Micro Lett.* **2023**, *15*, No. 124.
(18) Chen, X.; Wu, Y.; Shao, J.; Jiang, T.; Yu, A.; Xu, L.; Wang, Z. L. On-skin triboelectric nanogenerator and self-powered sensor with ultrathin thickness and high stretchability. *Small* **2017**, *13*, No. 1702929.
(19) Liu, T.; Liu, M.; Dou, S.; Sun, J.; Cong, Z.; Jiang, C.; Du, C.; Pu, X.; Hu, W.; Wang, Z. L. Triboelectric-nanogenerator-based soft energy-harvesting skin enabled by toughly bonded elastomer/hydrogel hybrids. *ACS Nano* **2018**, *12*, 2818−2826.
(20) Weng, W.; Yang, J.; Zhang, Y.; Li, Y.; Yang, S.; Zhu, L.; Zhu, M. A route toward smart system integration: from fiber design to device construction. *Adv. Mater.* **2020**, *32*, No. 1902301.
(21) Yang, W.; Gong, W.; Hou, C.; Su, Y.; Guo, Y.; Zhang, W.; Li, Y.; Zhang, Q.; Wang, H. All-fiber tribo-ferroelectric synergistic electronics with high thermal-moisture stability and comfortability. *Nat. Commun.* **2019**, *10*, No. 5541.
(22) Zhong, J.; Zhang, Y.; Zhong, Q.; Hu, Q.; Hu, B.; Wang, Z. L.; Zhou, J. Fiber-based generator for wearable electronics and mobile medication. *ACS Nano* **2014**, *8*, 6273−6280.
(23) Gong, W.; Hou, C.; Guo, Y.; Zhou, J.; Mu, J.; Li, Y.; Zhang, Q.; Wang, H. A wearable, fibroid, self-powered active kinematic sensor based on stretchable sheath-core structural triboelectric fibers. *Nano Energy* **2017**, *39*, 673−683.
(24) Ma, L.; Zhou, M.; Wu, R.; Patil, A.; Gong, H.; Zhu, S.; Wang, T.; Zhang, Y.; Shen, S.; Dong, K.; Yang, L.; Wang, J.; Guo, W.; Wang, Z. L. Continuous and scalable manufacture of hybridized nano-micro triboelectric yarns for energy harvesting and signal sensing. *ACS Nano* **2020**, *14*, 4716−4726.
(25) Li, Y.; Guo, F.; Hao, Y.; Gupta, S. K.; Hu, J.; Wang, Y.; Wang, N.; Zhao, Y.; Guo, M. Helical nanofiber yarn enabling highly stretchable engineered microtissue. *Proc. Natl. Acad. Sci. U.S.A.* **2019**, *116*, 9245−9250.
(26) Fu, K.; Zhou, J.; Wu, H.; Su, Z. Fibrous self-powered sensor with high stretchability for physiological information monitoring. *Nano Energy* **2021**, *88*, No. 106258.
(27) Lima, M. D.; Li, N.; Andrade, M. J. D.; Fang, S.; Oh, J.; Spinks, G. M.; Kozlov, M. E.; Haines, C. S.; Suh, D.; Foroughi, J.; Kim, S. J.; Chen, Y.; Ware, T.; Shin, M. K.; Machado, L. D.; Fonseca, A. F.; Madden, J. D.; Voit, W. E.; Galvão, D. S.; Baughman, R. H. Electrically, chemically, and photonically powered torsional and tensile actuation of hybrid carbon nanotube yarn muscles. *Science* **2012**, *338*, 928−932.
(28) Chen, P.; Xu, Y.; He, S.; Sun, X.; Pan, S.; Deng, J.; Chen, D.; Peng, H. Hierarchically arranged helical fibre actuators driven by solvents and vapours. *Nat. Nanotechnol.* **2015**, *10*, 1077−1083.
(29) Wang, R.; Fang, S.; Xiao, Y.; Gao, E.; Jiang, N.; Li, Y.; Mou, L.; Shen, Y.; Zhao, W.; Li, S.; Fonseca, A. F.; Galvão, D. S.; Chen, M.; He, W.; Yu, K.; Lu, H.; Wang, X.; Qian, D.; Aliev, A. E.; Li, N.; Haines, C. S.; Liu, Z.; Mu, J.; Wang, Z.; Yin, S.; Lima, M. D.; An, B.; Zhou, X.; Liu, Z.; Baughman, R. H. Torsional refrigeration by twisted, coiled, and supercoiled fibers. *Science* **2019**, *366*, 216−221.
(30) Marion, J. S.; Gupta, N.; Cheung, H.; Monir, K.; Anikeeva, P.; Fink, Y. Thermally drawn highly conductive fibers with controlled elasticity. *Adv. Mater.* **2022**, *34*, No. 2201081.
(31) Zhang, D.; Yang, W.; Gong, W.; Ma, W.; Hou, C.; Li, Y.; Zhang, Q.; Wang, H. Abrasion resistant/waterproof stretchable triboelectric yarns based on fermat spirals. *Adv. Mater.* **2021**, *33*, No. e2100782.
(32) Gao, Y.; Guo, F.; Cao, P.; Liu, J.; Li, D.; Wu, J.; Wang, N.; Su, Y.; Zhao, Y. Winding-locked carbon nanotubes/polymer nanofibers helical yarn for ultrastretchable conductor and strain sensor. *ACS Nano* **2020**, *14*, 3442−3450.
(33) Ye, C.; Dong, S.; Ren, J.; Ling, S. Ultrastable and high-performance silk energy harvesting textiles. *Nano-Micro Lett.* **2020**, *12*, No. 12.
(34) He, X.; Zi, Y.; Guo, H.; Zheng, H.; Xi, Y.; Wu, C.; Wang, J.; Zhang, W.; Lu, C.; Wang, Z. L. A highly stretchable fiber-based triboelectric nanogenerator for self-powered wearable electronics. *Adv. Funct. Mater.* **2017**, *27*, No. 1604378.
(35) Dong, K.; Deng, J.; Ding, W.; Wang, A. C.; Wang, P.; Cheng, C.; Wang, Y. C.; Jin, L.; Gu, B.; Sun, B.; Wang, Z. L. Versatile core−sheath yarn for sustainable biomechanical energy harvesting and real-time human-interactive sensing. *Adv. Energy Mater.* **2018**, *8*, No. 1801114.
(36) Xiao, R.; Yu, G.; Xu, B.; Wang, N.; Liu, X. Fiber surface/interfacial engineering on wearable electronics. *Small* **2021**, *17*, No. 2102903.
(37) Kim, S. H.; Lee, J. H.; Kim, J. W.; Lee, S. Y.; Park, S. J. Interfacial behaviors of basalt fiber-reinforced polymeric composites: A short review. *Adv. Fiber Mater.* **2022**, *4*, 1414−1433.
(38) Ning, C.; Cheng, R.; Jiang, Y.; Sheng, F.; Yi, J.; Shen, S.; Zhang, Y.; Peng, X.; Dong, K.; Wang, Z. L. Helical fiber strain sensors based on triboelectric nanogenerators for self-powered human respiratory monitoring. *ACS Nano* **2022**, *16*, 2811−2821.
(39) Wang, H.; Han, M.; Song, Y.; Zhang, H. Design, manufacturing and applications of wearable triboelectric nanogenerators. *Nano Energy* **2021**, *81*, No. 105627.
(40) Tao, X. Study of fiber-based wearable energy systems. *Acc. Chem. Res.* **2019**, *52*, 307−315.
(41) Huang, L.; Lin, S.; Xu, Z.; Zhou, H.; Duan, J.; Hu, B.; Zhou, J. Fiber-Based Energy Conversion Devices for Human-Body Energy Harvesting. *Adv. Mater.* **2020**, *32*, No. 1902034.
(42) Zhao, S.; Li, J.; Cao, D.; Zhang, G.; Li, J.; Li, K.; Yang, Y.; Wang, W.; Jin, Y.; Sun, R.; Wong, C. P. Recent advancements in flexible and stretchable electrodes for electromechanical sensors: strategies, materials, and features. *ACS Appl. Mater. Interfaces* **2017**, *9*, 12147−12164.
(43) Wang, Y.; Liu, F.; Wang, N.; Yue, G.; Wang, X.; Cai, B.; Hao, Y.; Li, Y.; Guo, F.; Zhang, Z.; Wang, S.; Guo, M.; Kong, L.; Zhao, Y.; Lei, J.; Zhao, Y. Bioinspired stretchable helical nanofiber yarn scaffold for locomotive tissue dynamic regeneration. *Matter* **2022**, *5*, 4480−4501.

https://doi.org/10.1021/acsnano.4c03115
ACS Nano XXXX, XXX, XXX−XXX